IEEE Access
Multidisciplinary ⋮ Rapid Review ⋮ Open Access Journal

Received December 29, 2020, accepted January 26, 2021, date of publication February 10, 2021, date of current version February 24, 2021.

Digital Object Identifier 10.1109/ACCESS.2021.3058506

Imperfections in Integrated Devices Allow the Emergence of Unexpected Strange Attractors in Electronic Circuits

MAIDE BUCOLO[1,2], (Senior Member, IEEE), ARTURO BUSCARINO[1,2], (Senior Member, IEEE), CARLO FAMOSO[1], (Member, IEEE), LUIGI FORTUNA[1,2], (Fellow, IEEE), AND SALVINA GAGLIANO[1]

[1]Dipartimento di Ingegneria Elettrica Elettronica e Informatica, University of Catania, 95125 Catania, Italy
[2]CNR-IASI, Italian National Research Council, Institute for Systems Analysis and Computer Science–Antonio Ruberti, 00185 Rome, Italy

Corresponding author: Arturo Buscarino (arturo.buscarino@unict.it)

This work was support by the Fondi di ateneo 2020-2022, Università di Catania, linea Open Access.

ABSTRACT The realization of integrated devices determines unavoidable imperfections which are linked to the manufacturing process, thus making them imperfect systems. Imperfection is not always detrimental, as it can lead to unexpected complex and organized behaviors. In this paper we explore the possibility of designing imperfect electronic circuits producing a chaotic flow with bandwidth up to the order to several megahertz thanks to the hidden dynamics induced by construction imperfections, and whose characteristics can be tuned by means of a single variable resistor, acting as bifurcation parameter. Moreover, a strategy to estimate the parameters of the hidden dynamics is devised and the synchronization of imperfect chaotic circuits is shown. The paper further remarks that imperfection can play an important role in the realization of robust chaos generators based on simple circuits.

INDEX TERMS Chaos, imperfect systems, non-ideality, nonlinear circuits, nonlinear dynamics.

I. INTRODUCTION

The design of electronic circuits able to generate nonlinear behavior and strange attractors is a topic deeply studied in literature since many decades [1], [2]. The fact that even the simplest autonomous ideal electronic system capable of generating chaos must encompass at least three memory elements and a nonlinear device is a well-established knowledge [3]. Recently, the possibility of observing chaotic dynamics in circuits made of fewer components have been explored by using memristive devices, which are memory and nonlinear elements [4], or by implementing simplified piecewise-linear functions [5]. Memristive circuits have been proposed with the aim of defining autonomous circuits with infinite coexisting attractors [6] or with asymmetric attractors [7], as well as associative memories with variable learning rates [8], keeping limited the complexity of the electronic implementations. Compact solutions have been also proposed for Boolean chaos generators in [9] and [10], where integrated devices based on CMOS technology are used.

In this paper we focus on compact circuits in which the occurrence of chaotic oscillations is observed thanks to nonidealities in integrated devices. It is well-known, in fact, that the very first examples of chaos in electronic circuits dates back to decades before the formal definition of chaos [11]. Parasitic effects and nonidealities, in fact, may lead to the occurrence of chaotic regimes even in circuits not intentionally designed to this purpose [12]. A diode, for example, is a nonlinear device that presents a parasitic capacitance and, in fact, one of the simplest electronic systems capable of generating chaos is an inductor-capacitor-diode circuit [13].

The integrated circuits are designed to guarantee performance for defined aims by using the suitable technology. Indeed, they are tested to ensure, with a given tolerance, the desired performance, in spite of the structural imperfections linked to the manufacturing process that include both nonlinearities and parasitic reactive elements. The design of the integrated devices using either CMOS or bipolar or modern silicon on insulator (SOI) and fin field-effect transistor (FInFET) technologies leads to imperfections that causes the generation of well-known parasitics linear and nonlinear circuit elements [14]. If on the one hand, parasitic nonlinearities represent an element of deterioration for the device, making it an *imperfect* element, on the other hand they can enhance its characteristics, enriching its dynamics and allowing the manifestation of behaviors that would otherwise not be observable [15], [16], even if parasitic memory elements

The associate editor coordinating the review of this manuscript and approving it for publication was Qiang Lai.

included in the integrated device and the related parameters cannot be directly modified.

Even if in a stock of the same electronic device, the same structural imperfections can be found, their parameters are randomly distributed. Therefore, in standard integrated devices, discovering these real hidden dynamics and the associated parameters is not straightforward. In fact, also the SPICE models of many integrated circuits do not allow to discover the hidden imperfect structures of the devices. It should be noted that the term hidden dynamics does not refer to the possibility of observing hidden attractors [17], but rather on the fact that the physical implementation of electronic circuits face unavoidable drifts from the ideal behavior. Moreover, the identification of such dynamics can be performed if it leads to the emergence of unexpected strange phenomena. In this case, the identification can be done by using non traditional techniques, thus allowing the possibility of exploiting the imperfections to reach complex behavior. An empirical approach based on the comparison with similar behaviors allows to characterize the complex behavior of circuits that include imperfect analog integrated devices.

Despite the fact that imperfect systems and devices are becoming a recurrent topic in the scientific literature, in this paper, it is emphasized the behavior of two simple electronic circuits whose basic element is a standard and imperfect integrated device. In [16], the occurrence of chaos in simple operational amplifier integrated circuits has been shown. The focus of this contribution is oriented towards other integrated devices whose imperfections are responsible of the onset of chaos and strange attractors and towards the possibility of unfolding this occurrence by deriving behavioral models based on optimization and synchronization approach [18].

We focus, therefore, on two different off-the-shelf integrated circuits, the LM311p and the TL084, whose realization is connected to unavoidable manufacturing imperfections with respect to the ideal model, which are the key ingredients to observe unexpected chaotic oscillations with a bandwidth up to several megahertz, thus allowing for the realization of two new simple chaos generators [2]. Moreover, we will show that a chaotic behavior can be still observed when using high precision current feedback operational amplifiers.

The paper is organized as follows. In Sec. II, the two circuits are presented in the framework of imperfect systems, showing the essential components adopted and the experimental results proving the onset of chaotic oscillations thanks to the imperfect dynamic are discussed. The strategy to estimate by analogy the parameters of the hidden imperfect dynamics is outlined in Sec.III, while simple strategies to synchronize two circuits in chaotic regime, in spite of the fact that chaos is generated thanks to the parasitic dynamics, are discussed in Sec. IV. Conclusive remarks are reported in Sec. V.

II. THE IMPERFECT DYNAMICS OF ELECTRONIC CIRCUITS

An imperfect system can be described by a set of interacting dynamical equations, one modeling the ideal dynamics of the system and one accounting for the hidden dynamics linked to unavoidable imperfections [12]. In general, considering autonomous continuous-time systems, the equations can be written as:

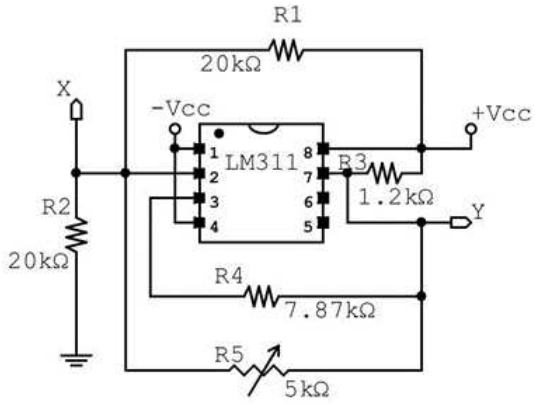

FIGURE 1. Schematic diagram of the electronic circuit with a voltage comparator that generates chaotic behaviors.

$$\begin{aligned} \dot{\mathrm{x}} &= \mathrm{f}(\mathrm{x}, \tilde{\mathrm{x}}, \mathrm{u}, \mathrm{w}, \mathrm{p}_1, t) \\ \dot{\tilde{\mathrm{x}}} &= \tilde{\mathrm{f}}(\mathrm{x}, \tilde{\mathrm{x}}, \mathrm{u}, \mathrm{w}, \mathrm{p}_1, t) \\ \mathrm{y} &= \eta(\mathrm{x}, \tilde{\mathrm{x}}, \mathrm{u}, \mathrm{w}, \mathrm{p}_2, t) \end{aligned} \tag{1}$$

where:

- $\mathrm{x} \in \mathbb{R}^n$ is the state vector of the system under ideal conditions;
- $\tilde{\mathrm{x}} \in \mathbb{R}^k$ is the state vector of the imperfect dynamics;
- $\mathrm{u} \in \mathbb{R}^m$ is the vector of the exogenous control signals;
- $\mathrm{w} \in \mathbb{R}^q$ is the vector of exogenous not controllable signals;
- $\mathrm{p}_1 \in \mathbb{R}_1^g$ and $\mathrm{p}_2 \in \mathbb{R}_2^g$ are the vectors of the system parameters;
- $\mathrm{y} \in \mathbb{R}^p$ is the vector of the outputs;

and $\mathrm{f} : \mathbb{R}^n \times \mathbb{R}^k \times \mathbb{R}^m \times \mathbb{R}^q \times \mathbb{R}_1^g \times \mathbb{R} \to \mathbb{R}^n$, $\tilde{\mathrm{f}} : \mathbb{R}^n \times \mathbb{R}^k \times \mathbb{R}^m \times \mathbb{R}^q \times \mathbb{R}_1^g \times \mathbb{R} \to \mathbb{R}^n$ and $\eta : \mathbb{R}^n \times \mathbb{R}^k \times \mathbb{R}^m \times \mathbb{R}^q \times \mathbb{R}_2^g \times \mathbb{R} \to \mathbb{R}^n$ are nonlinear vector fields. It should be remarked that we are considering hidden dynamics characterized by integer order derivatives, however a more general formalization of the imperfect systems may rely on fractional order systems and circuits [19].

The two imperfect circuits considered in this paper are both autonomous systems, therefore vectors u and w can be neglected.

The first circuit under investigation is based on the integrated device LM311p, manufactured by Texas Instruments. The circuit is implemented as in the schematic diagram reported in Fig. 1. The LM311p is a high speed differential voltage comparator. A voltage comparator is a circuit whose output voltage is a logic state that depends on the comparison between the voltage applied at the input (V_{in}) and a fixed threshold value (V_{REF}). The integrated device LM311p consists ideally in an operational amplifier performing the comparison of the input with the threshold and on a cascaded bipolar junction transistor implementing the logic

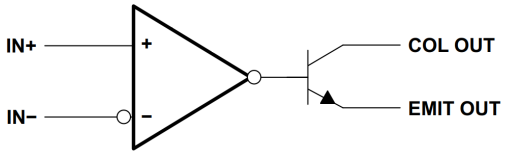

FIGURE 2. Ideal diagram of the LM311p integrated device.

output. The ideal scheme of the LM311p is reported in Fig. 2. The internal functional structure of the LM311p integrated device is reported in the block diagram shown in Fig. 3. As it can be noticed, no memory elements are explicitly taken into account, therefore all the capacitors are parasitic elements linked to the transistors and diodes included in the scheme, as a result of the imperfections linked to the manufacturing process. It should be noted, in particular, the output stage, realized through a transistor, providing a logic output.

Neither the ideal scheme, not the complete functional block diagram, explicitly contains memory elements. Therefore, a question arises: how chaos can emerge in such a circuit? In autonomous systems, deterministic chaos does appear only if at least three memory elements and a nonlinear element are included. Referring to Eqs. (1), we can reformulate them as follows for the case under consideration taking into account that, since no dynamics is explicitly included, the vector x does not exist:

$$\begin{aligned} \dot{\tilde{\mathrm{x}}} &= \tilde{\mathrm{f}}(\tilde{\mathrm{x}}, \mathrm{p}_1, t) \\ \mathrm{y} &= \eta(\tilde{\mathrm{x}}, \mathrm{p}_2, t) \end{aligned} \tag{2}$$

This representation allows to clearly identify the existence of an hidden dynamics which is the key ingredient for the onset of chaos.

The circuit is composed by few passive elements, including a variable resistor R_5. The supply voltage is fixed at the values $V_+ = 9.98\text{V}$ and $V_- = -3.99\text{V}$.

The emerging nonlinear dynamical behavior is investigated by varying the value of R_5, which acts as a bifurcation parameter for the system. We acquired the voltages at point as Y in Fig. 1, corresponding to the output of the integrated device by using a digital storage oscilloscope (Agilent DSOX4052A).

The nonlinear dynamics of the circuit has been examined ranging R_5 from 250Ω to 600Ω. Examples of the behaviors obtained are displayed in Tab. 1, where the reconstructed attractors, the temporal evolutions and the power spectral densities are reported.

It can be clearly seen that the signals for $R_5 = 338\Omega$ and $R_5 = 500\Omega$ have a fairly evident rich spectral component, while, for example, in the signals related to $R_5 = 258\Omega$ and $R_5 = 400\Omega$, a periodic behavior emerges predominantly. It should be also noted that the main frequency components can be found up to 10MHz. The bifurcation scenario under which the system goes by varying R_5 is shown in the experimental bifurcation diagram of Fig. 4. The bifurcation analysis has been carried out by acquiring the time-series obtained at each value of R_5 and then computing and plotting the local maxima and minima using Matlab®.

The embedding dimension m and the lag τ of the acquired time-series have been estimated by using the false nearest neighbor (FNN) algorithm discussed in [20] as $m = 3$ and $\tau = 5\mu\text{s}$. The largest Lyapunov exponent Λ_{max} has been evaluated by using the Rosenstein method [21]. In Fig. 5, Λ_{max} is reported as a function of R_5, thus showing the occurrence of windows of chaotic behavior, corresponding to positive values of Λ_{max}.

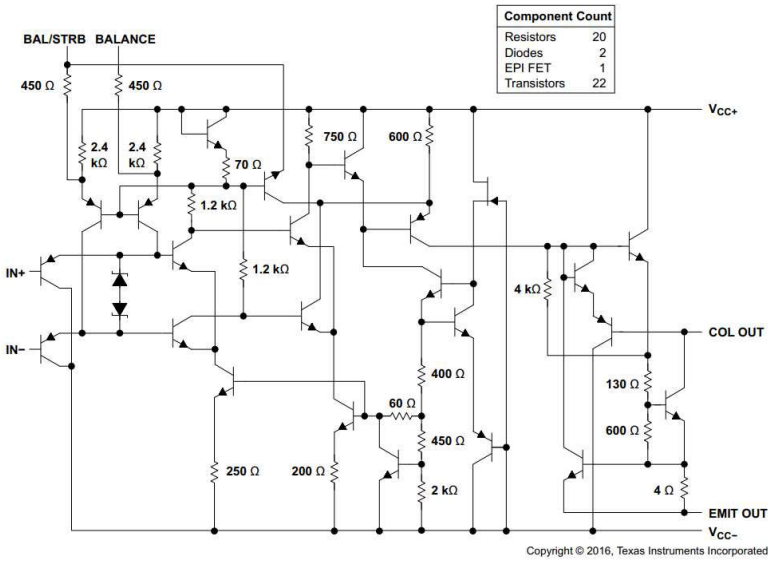

FIGURE 3. Schematic representation of the functional structure of the LM311p integrated device.

TABLE 1. Nonlinear dynamical behavior generated for different values of R_5 by the circuit with LM311p. From left to right: reconstructed attractors with lag $\tau = 5\mu$s, temporal behavior, frequency spectrum. From top to bottom: $R_5 = 258\Omega$, $R_5 = 338\Omega$, $R_5 = 400\Omega$, $R_5 = 500\Omega$, $R_5 = 608\Omega$.

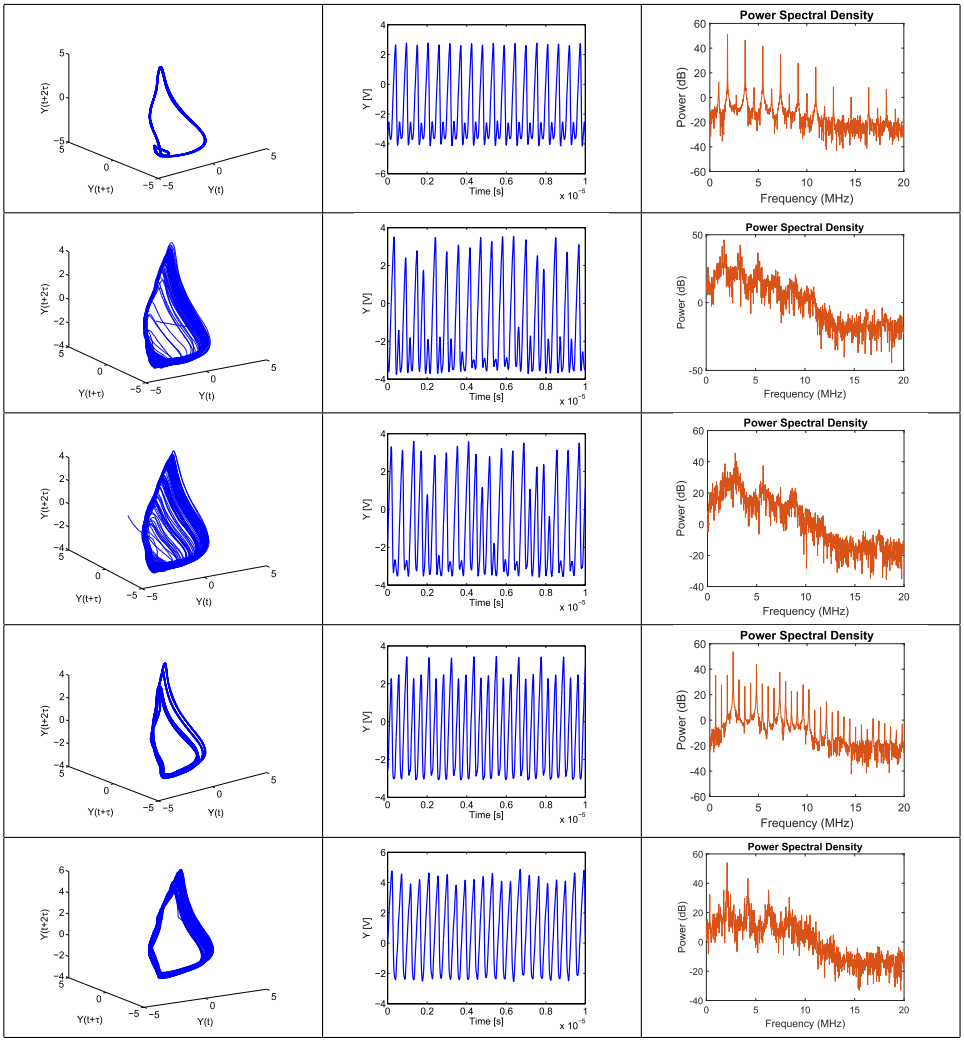

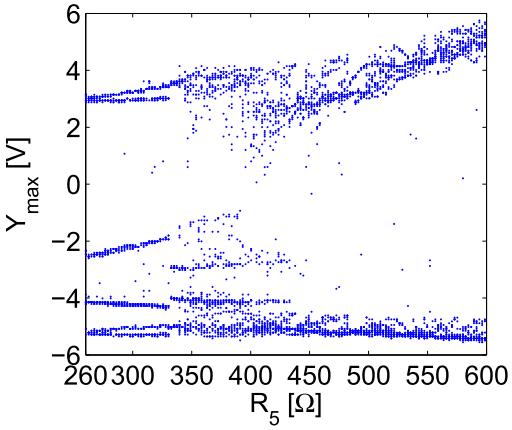

FIGURE 4. Experimental bifurcation diagram for the circuit in Fig. 1 varying resistor R_5.

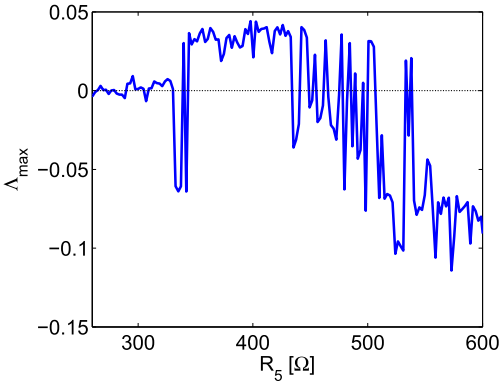

FIGURE 5. Largest Lyapunov exponent estimated for the circuit in Fig. 1 varying resistor R_5.

With a similar methodology, let us now examine a second circuit made combining a high-speed JFET input quad-operational amplifier integrated circuit TL084 and a NPN Darlington Power Transistor TIP122 manufactured by STMicroelectronics. The schematic of the circuit is shown in Fig. 6.

In this circuit only standard resistors and a single polyester film capacitor $C_1 = 100$nF are used. A voltage follower

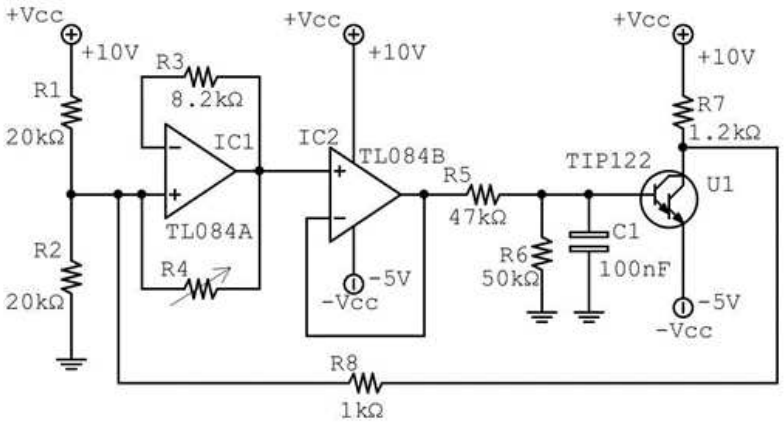

FIGURE 6. Schematic diagram of the electronic circuit with TL084 and TIP122 that generates chaotic behaviors.

TABLE 2. Nonlinear dynamical behavior generated for different values of R_4 by the circuit with TL084 and TIP122. From left to right: reconstructed attractors with $\tau = 5\mu$s, temporal behavior, frequency spectrum. From top to bottom: $R_4 = 82\Omega$, $R_4 = 89\Omega$, $R_4 = 92\Omega$, $R_4 = 104\Omega$, $R_4 = 120\Omega$.

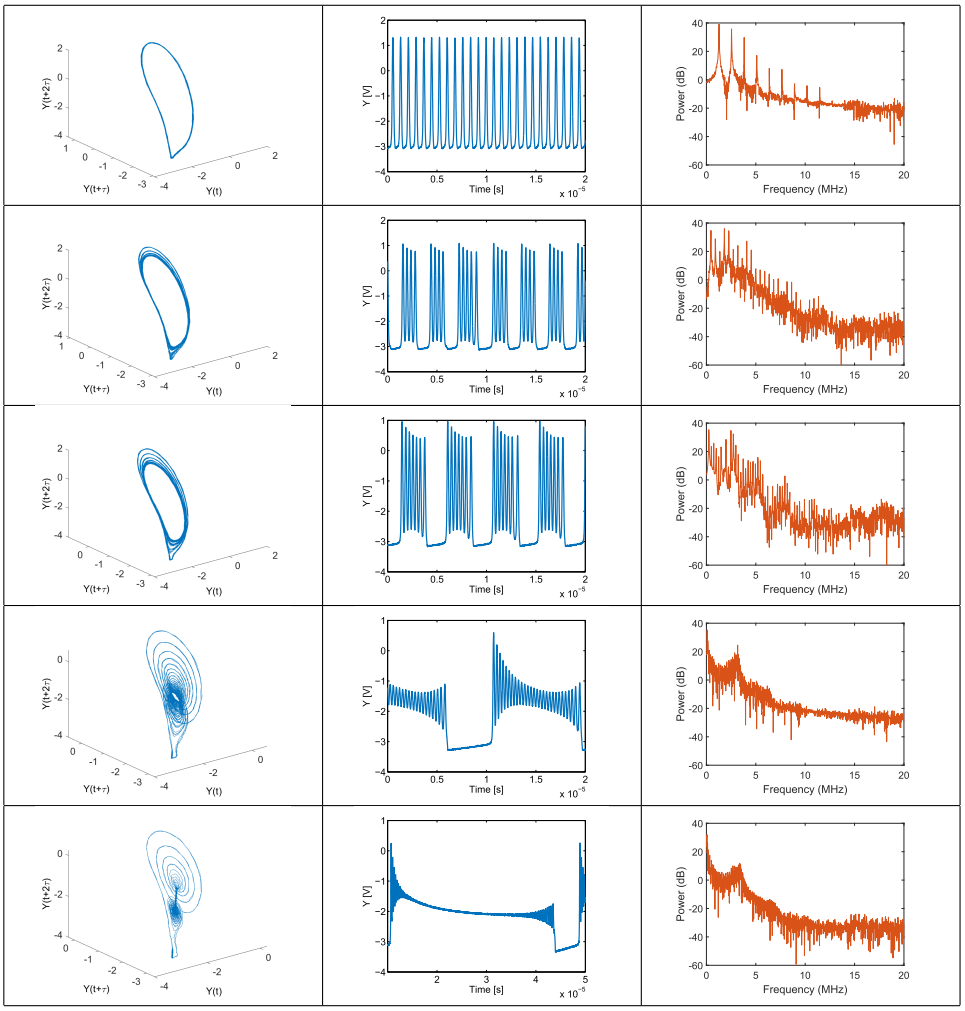

has been included in the circuit to separate the input of the transistor from the output of the previous stage of the operational amplifier. The supply voltage is fixed at the values $V_+ = 10$V and $V_- = -5$V. Similarly to the previous circuit, the number of memory elements physically included is lower than what expected to reach a chaotic behavior.

The nonlinear dynamical behavior of the circuit has been investigated varying the value of potentiometer R_4, realized

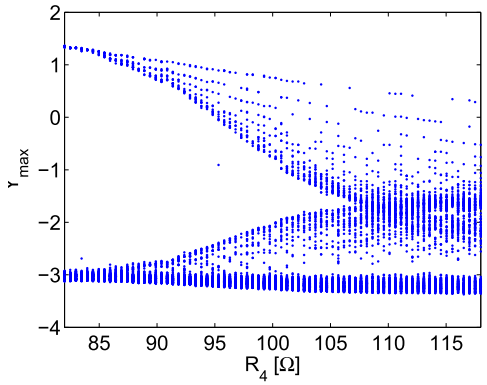

FIGURE 7. Experimental bifurcation diagram for the circuit in Fig. 6 varying resistor R_4.

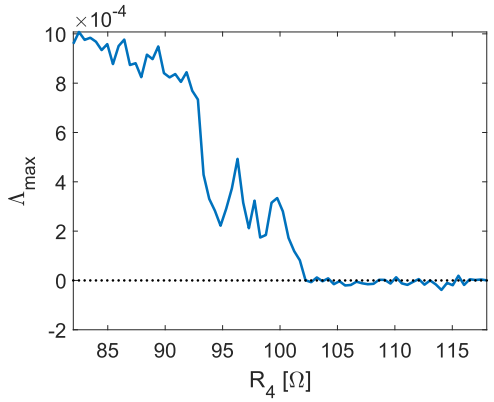

FIGURE 8. Largest Lyapunov exponent estimated for the circuit in Fig. 6 varying resistor R_4.

using a 1kΩ trimmer. We acquired the temporal evolution of the voltage at the collector of the TIP122 (labeled as Y) by using a digital storage oscilloscope (Agilent DSOX4052A).

The trimmer R_4 has been varied in the range from 82Ω to 118.5Ω, allowing to derive the rich repertoire of nonlinear dynamics exhibited by the circuit. The typical examples of reconstructed attractors and temporal behaviors of signals acquired are displayed in Tab. 2. Similarly to the previous case, the frequency spectra of the considered signals have been evaluated.

As it can be seen from the sequence of spectra, the dynamics of the system becomes increasingly richer as the value of R_4 varies within the established interval, moving from a chaotic flow to a periodic motion. Also for this circuit, the main frequency components are within a 10MHz bandwidth. The bifurcation route to chaos observed by varying R_4 is shown in the experimental bifurcation diagram of Fig. 7.

The largest Lyapunov exponent Λ_{max}, evaluated by using the Rosenstein method [21] with embedding dimension $m = 3$ and lag $\tau = 5\mu$s, is reported in Fig. 8 as a function of R_4, thus showing the occurrence of a bifurcation to chaos with decreasing values of R_4, where higher values of R_4 correspond to high frequency periodic oscillations. Moreover, varying the capacitor C_1 in the circuit in Fig. 6, does

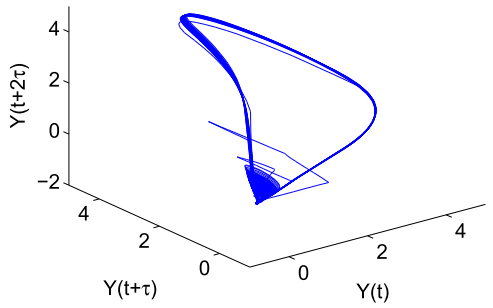

FIGURE 9. Reconstructed attractors generated for $R_4 = 90\Omega$ by the circuit with AD744 and TIP122 with $\tau = 5\mu$s.

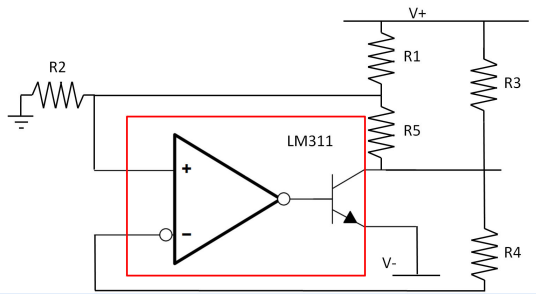

FIGURE 10. Analogy with the Colpitts chaotic oscillator of the circuit in Fig. 1 explicating the integrated device ideal scheme.

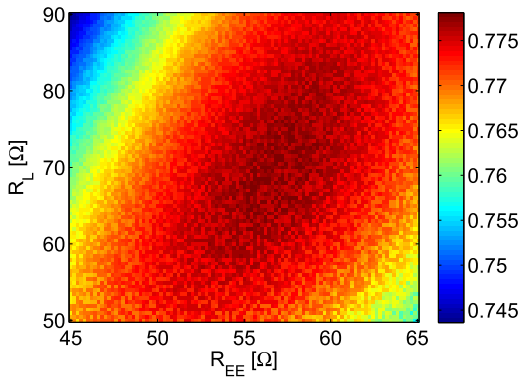

FIGURE 11. Normalized correlation coefficient between the data acquired from the circuit with $R_5 = 400\Omega$ and the variable V_{BE} obtained using the data acquired to drive the nonlinearity in Eq. (3).

not affect the frequency content of the obtained oscillations, thus stressing the fact that the hidden dynamics is the key ingredient leading to chaotic behavior.

Both bifurcation diagrams obtained for the two experimental circuits display a non trivial route to chaos, which is not the period doubling route typical of chaotic circuits [2]. Moreover, by looking at the circuits in Fig. 1 and Fig. 6, a question arises: can such circuits, without conservative elements and including insufficient explicit memory, produce the observed behavior? This must be related to the hidden imperfect dynamics of the integrated device.

Let us consider the same circuit reported in Fig. 6 substituting the TL084 with a current feedback operational amplifier

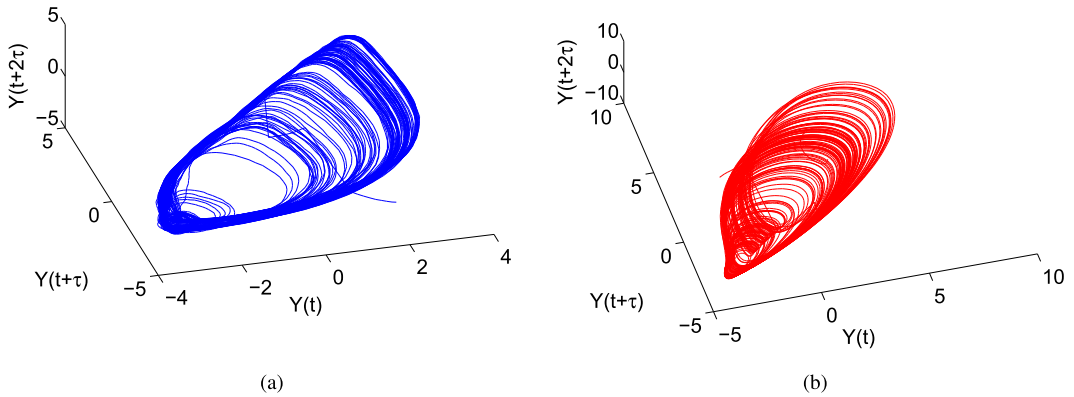

FIGURE 12. Chaotic attractor reconstruction for (a) the dataset obtained for $R_4 = 400\Omega$ and (b) the Colpitts oscillator for $C_1 = C_2 = 900$pF, $L = 1.64\mu$H, $R_L = 70\Omega$ and $R_{EE} = 56.6\Omega$.

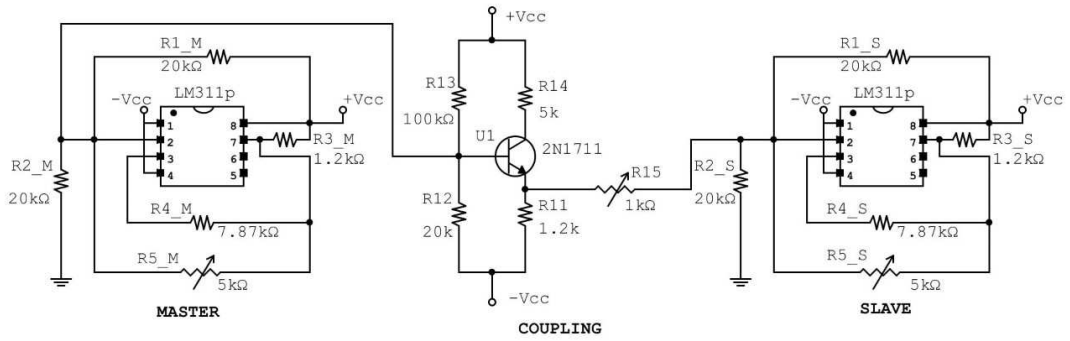

FIGURE 13. Schematic representation of the master-slave configuration for the synchronization of two circuits as in Fig. 1.

(CFOA). CFOAs are used in the realization of high-frequency chaotic circuits [22], [23] and present an high level of precision. We adopted an AD744 CFOA, with supply voltage fixed at the values $V_+ = 5$V and $V_- = -3$V. The embedding dimension and lag of the attractor observed for $R_4 = 90\Omega$ have been estimated as $m = 3$ and $\tau = 5\mu$s, and the phase space reconstruction is reported in Fig. 9. The largest Lyapunov exponent calculated as $\Lambda_{max} = 0.4 \cdot 10^{-4}$ confirms that a weak chaotic behavior can be retrieved. Even if the chaotic behavior is similar to that observed for the circuit with TL084, the bandwidth of the frequency spectrum appears to be limited below 1MHz. This is linked to the parasitic memory elements encompassed in the AD744, whose higher accuracy with respect to the TL084 leads to lower time constants. In general, the internal topology of the considered operational amplifier has a strong impact on the emerging behavior.

Therefore, the focus will be now oriented towards the possibility of deriving a behavioral model of the hidden dynamics of imperfect integrated devices.

III. ESTIMATING THE HIDDEN DYNAMICS OF IMPERFECT INTEGRATED DEVICE

In order to provide a qualitative model of the hidden dynamics responsible for the onset of chaos, we focus on the circuit based on the LM311p as we can refer by analogy its topology to a Colpitts-like oscillator [24] that, as shown in Fig. 10, share a similar circuit topology with the ideal scheme of the considered circuit and a similar chaotic attractor. The Colpitts oscillator is governed by the following set of dynamical equations:

$$\begin{aligned} C_1 \frac{dV_{CE}}{dt} &= I_L - I_C \\ C_2 \frac{dV_{BE}}{dt} &= -\frac{V_{EE} + V_{BE}}{R_{EE}} - I_L - I_B \\ L \frac{dI_L}{dt} &= V_{CC} - V_{CE} + V_{BE} - I_L R_L \end{aligned} \tag{3}$$

with

$$I_B = \begin{cases} 0 & \text{if } V_{BE} \geq V_{TH} \\ \dfrac{V_{BE} - V_{TH}}{R_{ON}} & \text{if } V_{BE} < V_{TH} \end{cases}$$

and $I_C = \beta_F I_B$, where $V_{TH} = 0.75$V is the threshold voltage, $R_{ON} = 100\Omega$ is the small-signal on-resistance of the base-emitter junction, and $\beta_F = 225.9$ is the forward current gain of the transistor, $V_{CC} = 9.98$V and $V_{EE} = -3.99$V.

In order to achieve a model matching with the observed behavior, the estimation of the Colpitts parameters in Eq. (3) is performed by using an approach based on the synchronization of chaotic dynamics [18]. It should be remarked that we

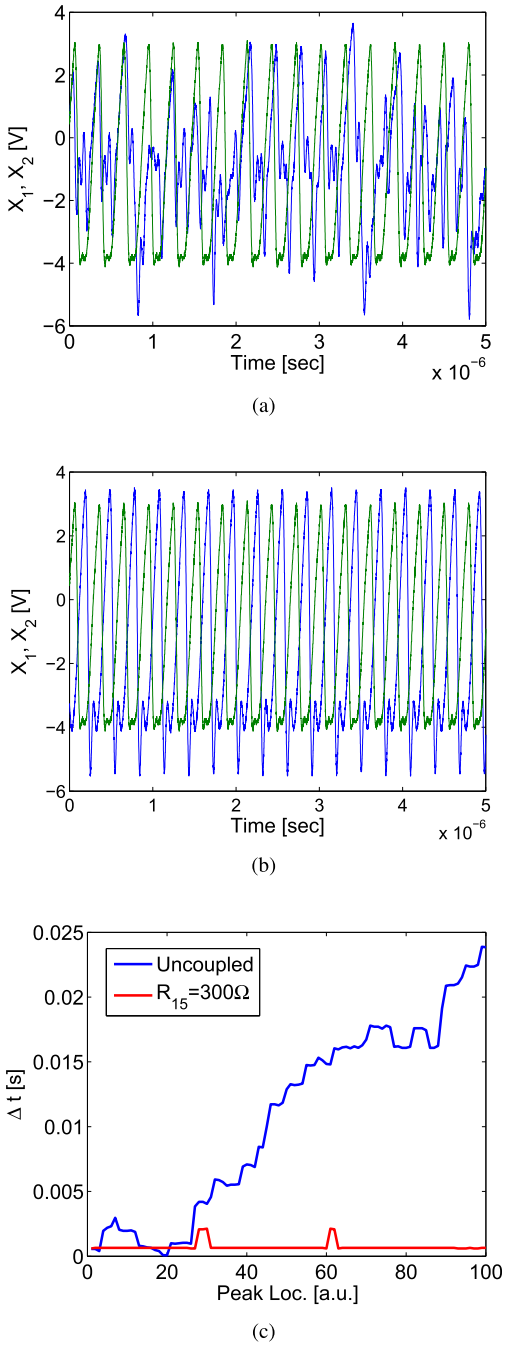

FIGURE 14. Master-slave synchronization of two circuits as in Fig. 1: (a) uncoupled dynamics of voltages at Y; (b) coupled dynamics with $R_{15} = 300\Omega$ (Green: master system; Blue: slave system) and (c) time lag between corresponding peaks in the master and in the slave.

rely on the dimensional Eq. (3) instead of providing dimensionless parameters in order to estimate the time-constant of the hidden dynamics on the basis of the parasitic capacitors included in the integrated device. The basic principle is to couple the experimental setup with a numerical simulation of Eq. (3) for different values of the equation parameters. In particular, the acquisitions performed on the circuit are used to drive the nonlinearity of Eq. (3) and the synchronization error is evaluated calculating the correlation coefficient between

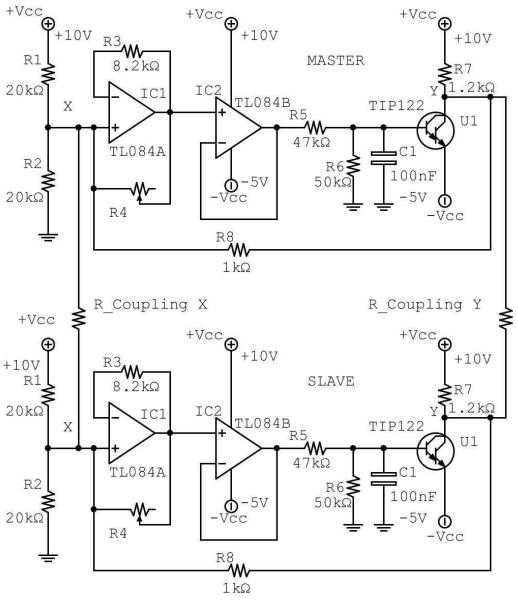

FIGURE 15. Schematic representation of the bidirectional diffusive coupling for the synchronization of two circuits as in Fig. 6.

the numerical simulation of variable V_{BE} and the experimental trends. When the parameters of the model are representative of the observed behavior, the correlation will reach the maximum value. Thus, we are using the Colpitts structure as an observer for the imperfect circuit. The parameter of the Colpitts observer are searched by using an optimization algorithm which maximizes the level of correlation.

The map reported in Fig. 11 reports the normalized correlation coefficient between experimental data and numerical simulations when the data used to drive the mathematical model is obtained for $R_5 = 400\Omega$. A cross-section of the Colpitts parameter space related to R_L and R_{EE} is investigated, considering constant the other parameters. The highest values of correlation can be retrieved around the point represented by $R_L = 70\Omega$ and $R_{EE} = 56.6\Omega$. The other parameters for Eq. (3) representative of the chaotic attractor observed for $R_5 = 400\Omega$, as reconstructed by using a time lag $\tau = 5\mu$s and reported in Fig. 12(a), are identified as $C_1 = C_2 = 900$pF, $L = 1.64\mu$H which lead to the attractor for the Colpitts oscillator reported in Fig. 12(b), reconstructed for comparison from variable V_{BE} with the same time lag $\tau = 5\mu$s.

The outlined strategy, therefore, can be considered in the framework of parameters estimation based on exploiting the intentional insertion of noise [25], with the main difference that imperfections are naturally present in real integrated devices.

IV. SYNCHRONIZATION OF NON-IDEAL CHAOTIC CIRCUITS

In spite of the fact that chaotic oscillations are highly influenced by their initial conditions, a wide literature exists on the synchronization of chaotic circuits [26]. Fewer results can be found that address the problem of synchronizing

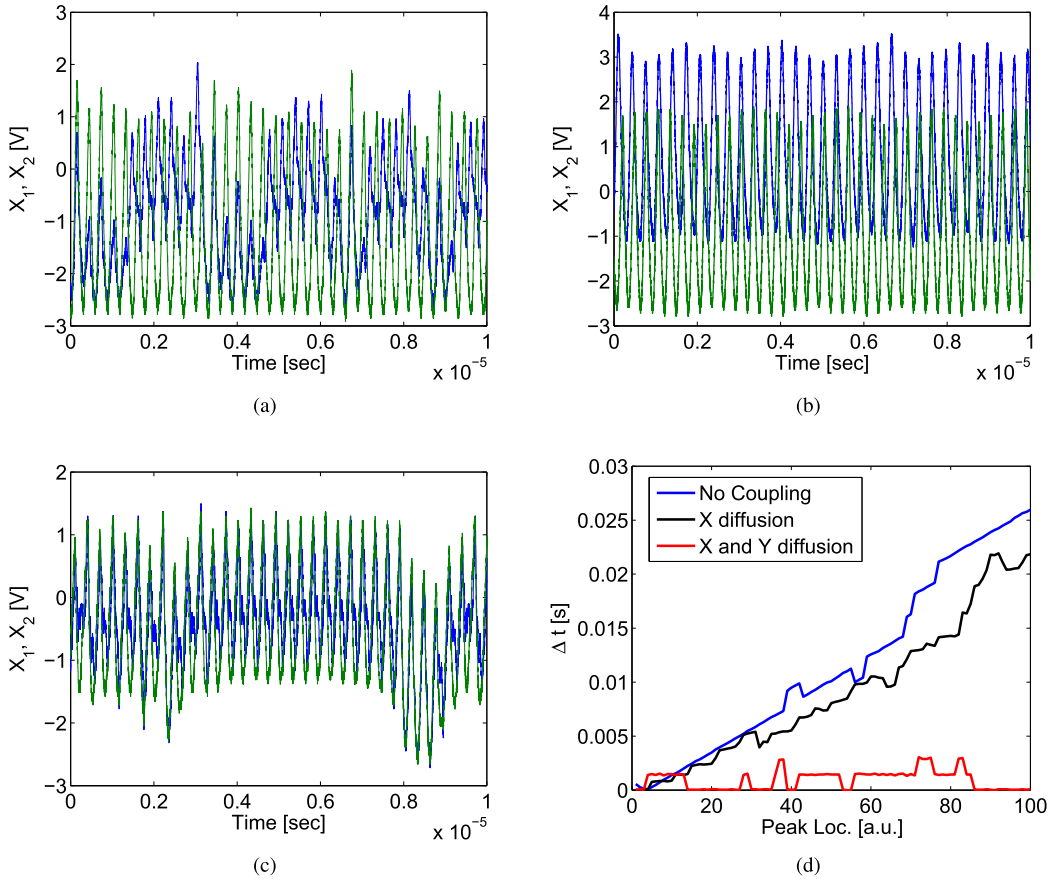

FIGURE 16. Diffusive synchronization of two circuits as in Fig. 6: (a) uncoupled dynamics of voltages at Y; (b) coupled dynamics with $R_X = 330\Omega$; (c) coupled dynamics with $R_X = 330\Omega$ and $R_Y = 10\Omega$ (Green: system 1; Blue: system 2) and (d) time lag between corresponding peaks in the two systems.

non-identical chaotic circuits and systems [27]. Here we focus on a much controversial scenario, since the synchronization of a pair of chaotic circuits as described above faces the problem that they are non-identical due to the nonidealities represented by parasitic elements in the integrated devices which may differ either within devices from the same stock.

When considering two different chaotic systems, a complete synchronization among the two dynamics cannot be reached. However, two non-identical chaotic systems can reach a weaker level of coordination and phase/lag synchronization can be often observed by using standard coupling schemes [28]. This condition implies that the two corresponding states are synchronized with a constant time lag.

In this Section, either adopting master-slave schemes or implementing a bidirectional coupling by using diffusive elements [28], we show that it is possible to synchronize pairs of chaotic circuits in which, besides tolerances of components, the non-ideal parasitic elements in the integrated devices are responsible for the occurrence of chaos.

Let us consider the coupling scheme reported in Fig. 13. It consists in a master-slave coupling for the circuit based on the LM311p integrated device, in which the master drives the slave by sending the X voltage through a network based on a standard 2N1711 transistor. The role of such network is to implement a monodirectional coupling with R_{15} determining the coupling strength. The level of synchronization obtained by using such scheme is definitely influenced by the fact that the two circuits are fundamentally different in the parasitic dynamics. However, an in-phase chaotic motion can be observed for values of R_{15} lower than 300Ω. Figure 14 shows the two cases of uncoupled and coupled dynamics for two circuits based on the LM311p. The time lag between peaks of the voltages at point Y of the two circuits is reported in Fig. 14(c) for the two cases of uncoupled and coupled dynamics. As it is possible to observe, the coupling induces an almost constant time lag between peaks in the master and in the slave circuit, thus showing the onset of lag synchronization.

The synchronization of two circuits based on the TL084 integrated device has been obtained by using a different coupling scheme, i.e. a bidirectional coupling based on diffusing voltages at points X and Y of the two coupled circuit as reported in Fig. 15. The coupling strength is governed by two coupling resistors R_X and R_Y implementing a diffusion between homologous voltages in the two circuits. The two diffusions are both necessary in order to observe a synchronous behavior, as shown in the temporal

evolution of voltages at node Y in the two circuits reported in Figs. 16(a), 16(b), and 16(c). A further proof of the onset of lag synchronization is shown in Fig. 16(d), where the time lag between peaks of the voltages at point Y of the two circuits is reported for the three cases of uncoupled dynamics, single diffusion and double diffusion. As it is possible to observe, the double diffusive coupling corresponds to an almost constant time lag between peaks in the two circuits.

V. CONCLUSION

In this paper we unveiled the occurrence of chaotic oscillation in electronic circuits based on standard off-the-shelf operational amplifiers by different manufacturers (Texas Instruments, STMicroelectronics). The presence of chaos has been observed in configurations in which passive resistors and integrated devices are mainly considered. The absence of a number of memory elements sufficient to obtain chaos proves that the parasitic dynamics of the integrated devices is the key ingredient for observing nonlinear and chaotic oscillations. Therefore, strange chaotic behavior does appear thanks to the imperfections related to the manufacturing process of the integrated devices

Even if the occurrence of chaos in operational amplifiers has been observed in previous papers [16], in this contribution we move forward from the experimental characterization of the chaotic behavior paying efforts to determine a strategy to outline behavioral models based on analogy, thus referring these cases to a wider class of systems where imperfections provide a richer behavior. Moreover, with respect to [16], in this paper we considered devices with logic and power applications, since the integrated packages include, or are coupled with, transistors and power Darlington configurations.

We characterized the dynamical behavior of two circuits based on the LM311p voltage comparator and on the operational amplifier TL084 coupled with a TIP122 Darlington transistor, showing several windows of chaotic behavior with main frequency components in the range of ten megahertz, by varying a single control parameter which leads the circuits through a bifurcation route which is more complex than the period doubling route typical of several chaotic circuits.

The observed behavior is robust to different samples of the same integrated device, even if slightly different chaotic and periodic oscillations are found, due to the unavoidable mismatches between samples obtained as a result of the same manufacturing process. In spite of this, the possibility to synchronize the chaotic dynamics arising from imperfections has been explored, showing that for the circuit based on the LM311p a master-slave configuration is able to coordinate the chaotic dynamics of two circuits, and for the circuit based on the TL084 and the TIP122 a bidirectional diffusion acting on two points of the coupled circuits is able to impress a synchronous chaotic motion. We also explored the possibility of using CFOAs, such as the AD744 integrated device, which are more robust and ensure higher level of precision. The circuit based on the AD744 led to the emergence of a weaker chaotic behavior, arguably due to the fact that they are designed to be more adherent to their ideal models, and the role of the hidden dynamics is therefore marginal.

The approach illustrated in this paper is, hence, based on hidden dynamics, for which a model cannot be easily established. A general strategy to derive qualitative models of the imperfect hidden dynamics responsible for the onset of chaos has been, therefore, outlined. The strategy is based on the principle of analogy and exploits the concept of modeling by synchronization. The hidden dynamics of the circuit based on the LM311p has been unveiled on the basis of an analogy with the well-known Colpitts oscillator and the parameters of the hidden dynamics have been estimated by synchronizing a Colpitts oscillator with the chaotic oscillations acquired from the experimental circuit. It is useful to remark that the approach is general and it can be proposed for other dynamics of circuits based on imperfect integrated devices.

Finally, we stress that the ease with which the proposed circuits can be realized and their negligible cost can certainly make them suitable to generate megahertz chaotic oscillations, without the use of additional capacitors or inductors, thus providing an effective example of a class of circuits in which imperfections can be intentionally exploited to obtain a specific task and providing a behavior robust with respect to the difference linked with the manufacturing process.

REFERENCES

[1] T. Matsumoto, L. O. Chua, and M. Komuro, "The double scroll," *IEEE Trans. Circuits Syst.*, vol. 32, no. 8, pp. 797–818, Aug. 1985.
[2] R. Madan, *Chua's Circuit: A Paradigm for Chaos*. Singapore: World Scientific, 1993.
[3] A. Sambas, S. Vaidyanathan, E. Tlelo-Cuautle, B. Abd-El-Atty, A. A. A. El-Latif, O. Guillen-Fernandez, Sukono, Y. Hidayat, and G. Gundara, "A 3-D multi-stable system with a peanut-shaped equilibrium curve: Circuit design, FPGA realization, and an application to image encryption," *IEEE Access*, vol. 8, pp. 137116–137132, 2020.
[4] B. Muthuswamy and L. O. Chua, "Simplest chaotic circuit," *Int. J. Bifurcation Chaos*, vol. 20, no. 05, pp. 1567–1580, May 2010.
[5] N. Wang, C. Li, H. Bao, M. Chen, and B. Bao, "Generating multi-scroll Chua's attractors via simplified piecewise-linear Chua's diode," *IEEE Trans. Circuits Syst. I, Reg. Papers*, vol. 66, no. 12, pp. 4767–4779, Dec. 2019.
[6] J. Sun, X. Zhao, J. Fang, and Y. Wang, "Autonomous memristor chaotic systems of infinite chaotic attractors and circuitry realization," *Nonlinear Dyn.*, vol. 94, no. 4, pp. 2879–2887, Dec. 2018.
[7] M. Hua, H. Wu, Q. Xu, M. Chen, and B. Bao, "Asymmetric memristive Chua's chaotic circuits," *Int. J. Electron.*, vol. 8, pp. 1–18, Oct. 2020.
[8] J. Sun, G. Han, Z. Zeng, and Y. Wang, "Memristor-based neural network circuit of full-function pavlov associative memory with time delay and variable learning rate," *IEEE Trans. Cybern.*, vol. 50, no. 7, pp. 2935–2945, Jul. 2019.
[9] M. Park, J. C. Rodgers, and D. P. Lathrop, "True random number generation using CMOS Boolean chaotic oscillator," *Microelectron. J.*, vol. 46, no. 12, pp. 1364–1370, Dec. 2015.
[10] J. M. Munoz-Pacheco, T. García-Chávez, V. R. Gonzalez-Diaz, G. de La Fuente-Cortes, and L. D. C. del Carmen Gómez-Pavón, "Two new asymmetric Boolean chaos oscillators with no dependence on incommensurate time-delays and their circuit implementation," *Symmetry*, vol. 12, no. 4, p. 506, Apr. 2020.
[11] M. Kennedy and L. Chua, "Van der Pol and chaos," *IEEE Trans. Circuits Syst.*, vol. 33, no. 10, pp. 974–980, Oct. 1986.
[12] M. Bucolo, A. Buscarino, C. Famoso, L. Fortuna, and M. Frasca, "Control of imperfect dynamical systems," *Nonlinear Dyn.*, vol. 98, no. 4, pp. 2989–2999, 2019.

[13] M. J. Hasler, "Electrical circuits with chaotic behavior," *Proc. IEEE*, vol. 75, no. 8, pp. 1009–1021, Aug. 1987.
[14] V. H. Carbajal-Gomez, E. Tlelo-Cuautle, J. M. Muñoz-Pacheco, L. G. de la Fraga, C. Sanchez-Lopez, and F. V. Fernandez-Fernandez, "Optimization and CMOS design of chaotic oscillators robust to PVT variations: INVITED," *Integration*, vol. 65, pp. 32–42, Mar. 2019.
[15] A. Buscarino, C. Corradino, L. Fortuna, M. Frasca, and J. C. Sprott, "Nonideal behavior of analog multipliers for chaos generation," *IEEE Trans. Circuits Syst. II, Exp. Briefs*, vol. 63, no. 4, pp. 396–400, Nov. 2015.
[16] G. Yim, J. Ryu, Y. Park, S. Rim, S. Lee, W. Kye, and C. Kim, "Chaotic behaviors of operational amplifiers," *Phys. Rev. E, Stat. Phys. Plasmas Fluids Relat. Interdiscip. Top.*, vol. 69, no. 4, 2004, Art. no. 045201.
[17] N. V. Kuznetsov and G. A. Leonov, "Hidden attractors in dynamical systems: Systems with no equilibria, multistability and coexisting attractors," *IFAC Proc. Volumes*, vol. 47, no. 3, pp. 5445–5454, 2014.
[18] R. Caponetto, L. Fortuna, M. Lavorgna, and G. Mangnaro, "Chaotic systems identification,"in *Genetic Algorithms in Engineering Systems*, A. Zalzala and P. Fleming, Eds. London, U.K.: The Institution of Electrical Engineers, 1997, pp. 118–133.
[19] E. Tlelo-Cuautle, A. D. Pano-Azucena, O. Guillen-Fernandez, and A. Silva-Juarez, *Analog/Digital Implementation of Fractional Order Chaotic Circuits and Applications*. Cham, Switzerland: Springer, 2020.
[20] R. Hegger and H. Kantz, "Improved false nearest neighbor method to detect determinism in time series data," *Phys. Rev. E, Stat. Phys. Plasmas Fluids Relat. Interdiscip. Top.*, vol. 60, no. 4, pp. 4970–4973, Oct. 1999.
[21] M. T. Rosenstein, J. J. Collins, and C. J. De Luca, "A practical method for calculating largest Lyapunov exponents from small data sets," *Phys. D, Nonlinear Phenomena*, vol. 65, nos. 1–2, pp. 117–134, May 1993.
[22] J. M. Muñoz-Pacheco, E. Tlelo-Cuautle, I. Toxqui-Toxqui, C. Sánchez-López, and R. Trejo-Guerra, "Frequency limitations in generating multi-scroll chaotic attractors using CFOAs," *Int. J. Electron.*, vol. 101, no. 11, pp. 1559–1569, Nov. 2014.
[23] F. Yu, P. Li, K. Gu, and B. Yin, "Research progress of multi-scroll chaotic oscillators based on current-mode devices," *Optik*, vol. 127, no. 13, pp. 5486–5490, Jul. 2016.
[24] M. P. Kennedy, "Chaos in the colpitts oscillator," *IEEE Trans. Circuits Syst. I, Fundam. Theory Appl.*, vol. 41, no. 11, pp. 771–774, Nov. 1994.
[25] J. Liu, F. Duan, F. Chapeau-Blondeau, and D. Abbott, "Exploring *Bona Fide* optimal noise for Bayesian parameter estimation," *IEEE Access*, vol. 8, pp. 18822–18831, 2020.
[26] L. M. Pecora and T. L. Carroll, "Synchronization in chaotic systems," *Phys. Rev. Lett.*, vol. 64, no. 8, p. 821, 1990.
[27] S. Boccaletti, J. Kurths, G. Osipov, D. L. Valladares, and C. S. Zhou, "The synchronization of chaotic systems," *Phys. Rep.*, vol. 366, nos. 1–2, pp. 1–101, 2002.
[28] A. Pikovsky, M. Rosenblum, and J. Kurths, "Phase synchronization in regular and chaotic systems," *Int. J. Bifurcation Chaos*, vol. 10, no. 10, pp. 2291–2305, Oct. 2000.

MAIDE BUCOLO (Senior Member, IEEE) received the M.S. degree in computer science engineering and the Ph.D. degree in electronic and control engineering from the University of Catania, in 1997 and 2001, respectively. During the Ph.D., she worked as a Research Scholar with the University of California San Diego (UCSD) and after that, often, she has been a Visiting Researcher with the Microhemodynamics Laboratory, Department of Bioengineering, UCSD. She is currently an Associate Professor of Control System with the Department of Electrical, Electronic and Informatics Engineering, University of Catania. In 2010, she established and became responsible of the Bio-Microfluidics Laboratory. She has been the coordinator of national projects and international exchange programs. She worked as an expert in the technology innovation demand of regional small and medium enterprisers. She is a President of the Master Course in Automation Engineering at Control of Complex Systems with the University of Catania. She has published more than 100 scientific contributions in peer-reviewed International Journals and Conferences. Her research interests include methodologies and low-cost technologies for bio-microfluidics systems modeling and control. She serves as an Associate Editor for IEEE TRANSACTIONS ON BIOMEDICAL CIRCUITS AND SYSTEMS.

ARTURO BUSCARINO (Senior Member, IEEE) graduated in computer science engineering, in 2004. He received the Ph.D. degree in electronics and automation engineering from the University of Catania, Italy, in 2008. He is currently a Research Associate with the University of Catania, he teaches Modeling and Optimization at the Laura Magistrale in Management Engineering and Automatic Control and at the Laurea in Electronics Engineering with the University of Catania. He works on nonlinear circuits, control, and synchronization. He published more than 165 papers on refereed international journals and international conference proceedings. His scientific research interests include nonlinear systems and chaos, complex networks, control systems, cellular nonlinear networks, and plasma engineering.

CARLO FAMOSO (Member, IEEE) received the M.S. degree in electronic engineering and the Ph.D. degree in complex systems from the Università degli Studi di Catania, Catania, Italy, in 2012 and 2015, respectively. Since 2012, he has been with the Dipartimento di Ingegneria Elettrica, Elettronica e Informatica, Università di Catania, where he currently teaches Calculus. He has coauthored several scientific articles and books. His current research interests include complex systems and soft sensors.

LUIGI FORTUNA (Fellow, IEEE) received the degree in electrical engineering *(cum laude)* from the University of Catania, Italy, in 1977. He was the Coordinator of the courses in electronic engineering and the Head of the Dipartimento di Ingegneria Elettrica Elettronica e dei Sistemi. From 2005 to 2012, he was the Dean of the Engineering Faculty. He is currently a Full Professor of System Theory with the University of Catania. He also teaches automatic control and robust control. He has published more than 500 technical articles and twelve scientific books. His scientific research interests include robust control, nonlinear science and complexity, chaos, cellular neural networks, softcomputing strategies for control, robotics, micronanosensor and smart devices for control, and nanocellular neural networks modeling. He was the IEEE Circuits and Systems (CAS) Chairman of the CNN Technical Committee, the IEEE CAS Distinguished Lecturer, from 2001 to 2002, and the IEEE Chairman of the IEEE CAS Chapter Central-South Italy.

SALVINA GAGLIANO received the M.S. degree in electrical engineering and the Ph.D. degree in electrical engineering from the Università degli Studi di Catania, Italy, in 2002 and 2006, respectively. Since 2006, she has carried out Scientific Research with the Dipartimento di Ingegneria Elettrica, Elettronica e Informatica, where she's currently teaching in Systems Theory for the Computer Engineering Degree Course. Before teaching systems theory, she was teaching Automatic Controls at the degree course in Industrial Engineering. She is also a Research Fellow with the University of Catania. She has coauthored several scientific articles and books. Her research activity has developed in the last two years in the study of microfluidic processes and control techniques.